Analytical calculation of nuclear magnetic resonance indirect spin–spin coupling constants at the generalized gradient approximation and hybrid levels of density-functional theory

Trygve Helgaker,[a] Mark Watson, and Nicholas C. Handy
Department of Chemistry, University of Cambridge, Lensfield Road, CB2 1EW United Kingdom

(Received 27 July 2000; accepted 11 September 2000)

A fully analytical implementation of the nuclear magnetic resonance (NMR) indirect nuclear spin–spin coupling constants at the density-functional theory (DFT) level is presented. The implementation involves all four contributions of the nonrelativistic Ramsey theory: The dia- and para-magnetic spin–orbit contributions as well as the paramagnetic Fermi-contact and spin–dipole contributions. Three different exchange-correlation functionals—LDA (local density approximation), BLYP (Becke–Lee–Yang–Parr), and B3LYP (hybrid BLYP)—are tested by comparison with experiment and high-level *ab initio* calculations for a series of molecules containing first-row elements. All three levels of theory represent a significant improvement on restrictred Hartree–Fock (RHF) theory in the sense that the RHF instability problems are absent in DFT. Also, there is a steady improvement in the quality of the calculated spin–spin couplings in the sequence LDA, BLYP, and B3LYP. For the first-row molecules investigated by us, the hybrid B3LYP functional performs particularly well, with errors similar to those observed at the best *ab initio* levels of theory. © *2000 American Institute of Physics.* [S0021-07-7(90)31545-3]

I. INTRODUCTION

The indirect nuclear spin–spin coupling constants are one of the central parameters that characterize high-resolution nuclear magnetic resonance (NMR) spectra. Within the Born–Oppenheimer approximation, these constants may be calculated as time-independent second-order molecular properties, where the perturbations are the magnetic fields generated by the stationary nuclei.[1] In practice, however, the accurate calculation of spin–spin coupling constants has proved to be considerably more difficult than the calculation of other second-order properties such as quadratic force constants, polarizabilities, magnetizabilities, and nuclear shielding constants.[2] The reasons for these difficulties are the following.

First, at the nonrelativistic level, several distinct mechanisms contribute to the spin–spin couplings:[1] The diamagnetic spin–orbit (DSO) mechanism, the paramagnetic spin–orbit (PSO) mechanism, the Fermi-contact (FC) mechanism, and the spin–dipole (SD) mechanism. All mechanisms may be important and none can be *a priori* neglected; programming and computational efforts increase accordingly. Second, the indirect spin–spin coupling constants involve triplet perturbations, whose accurate calculation requires a highly flexible description of the electronic system. The Hartree–Fock model, in particular, gives notoriously poor results and is often in error by an order of magnitude, rendering this basic model of *ab initio* theory useless for the calculation of spin–spin coupling constants; as a result, there are currently no levels of *ab initio* theory available for the calculation of spin–spin coupling constants of large systems. Third, the often dominant FC contribution to the spin–spin coupling depends critically on the electron density at the nuclei; the basis-set convergence is consequently slow and large sets must be employed for the results to be useful.

As a consequence, the calculation of NMR indirect spin–spin coupling constants is much less widespread than the calculation of NMR shielding constants, even though both sets of parameters are needed for a fully theoretical description of NMR spectra. The purpose of the present paper is to investigate the usefulness of density-functional theory (DFT) for the calculation of spin–spin coupling constants. In view of the success of the DFT methodology in recent years, it would in particular be interesting to see how DFT performs vis-à-vis the best *ab initio* methods with respect to the calculation of spin–spin coupling constants.

There have been several previous attempts at the calculation of spin–spin coupling constants at the DFT level. The first successful implementations are those of Malkin, Malkina and Salahub from 1994[3] and by Dickson and Ziegler from 1996.[4] The pioneering studies of these authors have been encouraging. In particular, their results demonstrated that DFT does not suffer from the triplet-instability problems that have plagued the application of Hartree–Fock theory to the calculation of spin–spin coupling constants; it is well established that the use of the random-phase approximation (RPA) Hartree–Fock approach often gives poor singlet-to-triplet excitation energies, whereas there are now ample results to show that the equivalent DFT calculations give much more accurate values for these excitation energies.[5] Moreover, Malkin *et al.*[3] and Dickson and Ziegler[4] also demonstrated that the accuracy achieved by DFT with respect to spin–spin coupling constants is sufficiently high to be useful in the application of DFT to the solution of chemical problems in NMR.

[a]Permanent address: Department of Chemistry, University of Oslo, P.O.B. 1033, Blindern, N-0315 Oslo, Norway. Electronic mail: trygve.helgaker@kjemi.uio.no

Nevertheless, some limitations of the studies by Malkin *et al.* and by Dickson and Ziegler prompted us to undertake this study. First, both studies ignored the sometimes important SD contribution to the spin–spin coupling constants; second, their applications were restricted to the local-density approximation (LDA) and generalized gradient approximation (GGA) levels of theory; third, both implementations were mixed analytical/finite difference implementations, reducing their overall efficiency. In our work, we calculate all four terms analytically, using standard response-theory methods; moreover, in addition to LDA[6] and BLYP (Becke–Lee–Yang–Parr),[7,8] our implementation includes the hybrid functional B3LYP (three-parameter hybrid BLYP).[9,10] In view of the success of the B3LYP functional for the calculation of molecular structure and energetics—for which it matches high-level *ab initio* methods—it would be interesting to see if a similar level of accuracy is achieved by hybrid methods in the calculation of spin–spin coupling constants.

In the final stages of this project, we became aware of a similar study by Ziegler and co-workers.[11] Very recently, these authors have presented a fully analytical implementation of DFT for the relativistic calculation of the indirect spin–spin coupling constants at the LDA and GGA levels of theory. Apart from being nonrelativistic, our treatment differs from theirs in the use of Gaussian-type orbitals rather than Slater-type orbitals and in that we are able to include exact Hartree–Fock exchange in our calculations. As will become apparent in this work, the inclusion of exact exchange is essential in order to achieve an accuracy that matches that of the best *ab initio* methods—at least for the organic molecules containing first-row atoms as studied by us.

II. THEORY AND IMPLEMENTATION

In the present section, we first review Ramsey's expression for the indirect spin–spin coupling constants;[1] next, we briefly consider the evaluation of these coupling constants in response theory; finally, we consider the implementation of DFT spin–spin coupling constants in DALTON.[12]

A. Ramsey's expression

In the present work, the indirect spin–spin coupling constants are evaluated as derivatives of the electronic energy. To summarize, we recall that the nuclear magnetic moments $\mathbf{M}_K$ are related to the nuclear spins $\mathbf{I}_K$ as

$$\mathbf{M}_K = \gamma_K \hbar I_K , \tag{1}$$

where the γ_K are the nuclear magnetogyric ratios. The normal and reduced nuclear indirect spin–spin coupling constants $\mathbf{J}_{KL}$ and $\mathbf{K}_{KL}$ may then be calculated as the total derivatives of the energy with respect to the nuclear magnetic moments as follows:

$$\mathbf{J}_{KL} = h \frac{\gamma_K}{2\pi} \frac{\gamma_L}{2\pi} \mathbf{K}_{KL} = h \frac{\gamma_K}{2\pi} \frac{\gamma_L}{2\pi} \frac{d^2 E}{d\mathbf{M}_K d\mathbf{M}_L} . \tag{2}$$

In the Born–Oppenheimer approximation, the nonrelativistic Hamiltonian takes the following form in the presence of nuclear magnetic moments (atomic units):

$$H = \frac{1}{2} \sum_i \left[\mathbf{p}_i + \mathbf{A}(\mathbf{r}_i)\right] \cdot \left[\mathbf{p}_i + \mathbf{A}(\mathbf{r}_i)\right] + \sum_i \mathbf{s}_i \cdot \mathbf{B}(\mathbf{r}_i) + V_{en} + V_{ee} + V_{nn} , \tag{3}$$

where $\mathbf{p}_i$ is the conjugate momentum of electron i and $\mathbf{s}_i$ its spin. In the point-charge model of the atomic nuclei, the vector potential $\mathbf{A}(\mathbf{r}_i)$ and its induction $\mathbf{B}(\mathbf{r}_i) = \nabla \times \mathbf{A}(\mathbf{r}_i)$ are given by

$$\mathbf{A}(\mathbf{r}_i) = \alpha^2 \sum_K \frac{\mathbf{M}_K \times \mathbf{r}_{iK}}{r_{iK}^3} , \tag{4}$$

$$\mathbf{B}(\mathbf{r}_i) = \frac{8\pi\alpha^2}{3} \sum_K \delta(\mathbf{r}_{iK}) \mathbf{M}_K + \alpha^2 \sum_K \frac{3\mathbf{r}_{iK}\mathbf{r}_{iK}^T - r_{iK}^2 \mathbf{I}_3}{r_{iK}^5} \mathbf{M}_K , \tag{5}$$

where α is the fine-structure constant and $\mathbf{r}_{iK}$ is the position of electron i relative to nucleus K. Inserting the nuclear vector potential (4) and the induction (5) in the electronic Hamiltonian (3) and rearranging, we obtain

$$H = \frac{1}{2} \sum_i p_i^2 + V_{en} + V_{ee} + V_{nn} + \sum_{KL} \mathbf{M}_K^T \mathbf{h}_{KL}^{\mathrm{DSO}} \mathbf{M}_L + \sum_K \mathbf{M}_K^T \mathbf{h}_K^{\mathrm{PSO}} + \sum_K \mathbf{M}_K^T (\mathbf{h}_K^{\mathrm{FC}} + \mathbf{h}_K^{\mathrm{SD}}) , \tag{6}$$

where we have introduced the diamagnetic spin–orbit (DSO) and paramagnetic spin–orbit (PSO) operators

$$\mathbf{h}_{KL}^{\mathrm{DSO}} = \frac{\alpha^4}{2} \sum_i \frac{(\mathbf{r}_{iK}^T \mathbf{r}_{iL}) \mathbf{I}_3 - \mathbf{r}_{iK} \mathbf{r}_{iL}^T}{r_{iK}^3 r_{iL}^3} , \tag{7}$$

$$\mathbf{h}_K^{\mathrm{PSO}} = \alpha^2 \sum_i \frac{\mathbf{r}_{iK} \times \mathbf{p}_i}{r_{iK}^3} , \tag{8}$$

as well as the triplet Fermi-contact (FC) and spin–dipole (SD) operators

$$\mathbf{h}_K^{\mathrm{FC}} = \frac{8\pi\alpha^2}{3} \sum_i \delta(\mathbf{r}_{iK}) \mathbf{s}_i , \tag{9}$$

$$\mathbf{h}_K^{\mathrm{SD}} = \alpha^2 \sum_i \frac{3(\mathbf{s}_i^T \mathbf{r}_{iL}) \mathbf{r}_{iK} - r_{iK}^2 \mathbf{s}_i}{r_{iK}^5} . \tag{10}$$

In the traditional sum-over-states formulation of molecular properties, this leads to the following Ramsey expression for the reduced spin–spin coupling constants:[1]

$$\mathbf{K}_{KL} = \langle 0 | \mathbf{h}_{KL}^{\mathrm{DSO}} | 0 \rangle + 2 \sum_{s>0} \frac{\langle 0 | \mathbf{h}_K^{\mathrm{PSO}} | s \rangle \langle s | \mathbf{h}_L^{\mathrm{PSO}} | 0 \rangle^T}{E_0 - E_s} + 2 \sum_t \frac{\langle 0 | \mathbf{h}_K^{\mathrm{FC}} + \mathbf{h}_K^{\mathrm{SD}} | t \rangle \langle t | \mathbf{h}_L^{\mathrm{FC}} + \mathbf{h}_L^{\mathrm{SD}} | 0 \rangle^T}{E_0 - E_t} , \tag{11}$$

where the first summation is over all singlet states different from the reference state and the second summation over all triplet states. Although this expression clearly expresses the different mechanisms that contribute to the spin–spin coupling constants in the conventional formalism of time-

independent perturbation theory, it is not useful for calculations since it requires a summation of the full set of excited states (which are anyway not accessible in DFT). In practice, the spin–spin coupling constants are evaluated as a second-order property according to (2), using the standard procedures for linear response theory.

B. Response theory

To outline the response-function approach to the calculation of spin–spin coupling constants,[2] we write the Kohn–Sham closed-shell energy in the form $E(\mathbf{M}_K,\boldsymbol{\lambda}_S,\boldsymbol{\lambda}_T)$ where the $\mathbf{M}_K$ are the nuclear magnetic moments, and where $\boldsymbol{\lambda}_S$ and $\boldsymbol{\lambda}_T$ are two sets of parameters that represent singlet and triplet variations in the electronic state. For the optimized energy, $\boldsymbol{\lambda}_S$ and $\boldsymbol{\lambda}_T$ are both zero. The reduced spin–spin coupling constants may now be calculated as

$$\mathbf{K}_{KL}=\frac{d^2E}{d\mathbf{M}_K d\mathbf{M}_L}=\frac{\partial^2 E}{\partial\mathbf{M}_K\partial\mathbf{M}_L}+\frac{\partial^2 E}{\partial\mathbf{M}_K\partial\boldsymbol{\lambda}_S}\frac{\partial\boldsymbol{\lambda}_S}{\partial\mathbf{M}_L}+\frac{\partial^2 E}{\partial\mathbf{M}_K\partial\boldsymbol{\lambda}_T}\frac{\partial\boldsymbol{\lambda}_T}{\partial\mathbf{M}_L}, \tag{12}$$

where all derivatives are evaluated for the optimized energy. The derivatives of $\boldsymbol{\lambda}_S$ and $\boldsymbol{\lambda}_T$ with respect to $\mathbf{M}_L$ are obtained by solving the response equations

$$\frac{\partial^2 E}{\partial\boldsymbol{\lambda}_S\partial\boldsymbol{\lambda}_S}\frac{\partial\boldsymbol{\lambda}_S}{\partial\mathbf{M}_L}=-\frac{\partial^2 E}{\partial\boldsymbol{\lambda}_S\partial\mathbf{M}_L}, \tag{13}$$

$$\frac{\partial^2 E}{\partial\boldsymbol{\lambda}_T\partial\boldsymbol{\lambda}_T}\frac{\partial\boldsymbol{\lambda}_T}{\partial\mathbf{M}_L}=-\frac{\partial^2 E}{\partial\boldsymbol{\lambda}_T\partial\mathbf{M}_L}, \tag{14}$$

where the symmetric matrices on the left-hand sides are the singlet and triplet electronic Hessians, respectively. Whereas the solution to the singlet equations (13) represents the perturbing influence of the imaginary singlet PSO operator, the solution to the triplet equations (14) represents the influence of the real triplet FC+SD operator; for symmetry reasons, there is no coupling between the singlet and triplet perturbations. The real singlet DSO operator enters the reduced coupling constant via the first term in (12) and requires no solution of linear equations.

The dimension of the imaginary singlet equations (13) is equal to the number of parameters in $\boldsymbol{\lambda}_S$—that is, to the number of occupied MOs times the number of unoccupied MOs. This dimension is sufficiently large that the equations are solved iteratively, without constructing the Hessian. There are three equations to be solved for each paramagnetic nucleus—that is, one equation for each Cartesian component of the PSO operator (8). The solution of these imaginary singlet equations follows the same scheme as the solution of the response equations for the calculation of chemical shieldings—see, for example, Ref. 2.

The solution of the real triplet equations (14) is more difficult since, because of the three components of each triplet state, the number of parameters in $\boldsymbol{\lambda}_T$ is three times the number of parameters in $\boldsymbol{\lambda}_S$. The triplet components do not mix, however, reducing each of the three equations for each nucleus to three separate smaller equations. In total, therefore, there are nine triplet equations to be solved for each nucleus, each of the same dimension as the singlet equations (13). By use of the Wigner–Eckart theorem, it is possible to reduce the number of independent equations for each nucleus to six, although this has not been done in our implementation. Moreover, we treat the FC and SD contributions separately since the additional cost is small (there is only one independent FC equation for each nucleus due to the high symmetry of the FC operator) and since this gives useful additional information about the transmission of the coupling (either as FC or SD).

In short, we solve 13 linear equations for each paramagnetic nucleus: Three imaginary singlet equations involving the PSO operator, one real triplet equation involving the FC operator, and nine real triplet equations involving the SD operator. This situation should be compared with the calculation of shieldings, for which we never solve more than three imaginary singlet equations for each molecule (one for each direction of the external magnetic field). In many cases, the FC contribution dominates the spin–spin couplings. Since this contribution requires only one set of linear equations to be solved for each nucleus, it is tempting to drop the remaining contributions. Unfortunately, it is impossible to predict with any certainty when the non-FC contributions may be neglected and all terms should, therefore, be included in the calculations.

C. Implementation in DALTON

Our implementation of NMR indirect spin–spin coupling constants is based on a previous such implementation at the Hartree–Fock and MCSCF (multiconfiguration self-consistent field) levels in DALTON[13] and on a recently described implementation of DFT shieldings in DALTON.[14] The implementation of DFT in DALTON is based on that in CADPAC,[15] using the same routines for generating the abscissas and weights of the density quadrature and for the functionals. The optimized DFT energies are, therefore, identical to those of CADPAC. Moreover, the present implementation of DFT in DALTON is preliminary in that it does not utilize point-group symmetry; also, there is no efficient screening of quadrature points and of the contributions from the individual orbitals at each point. There are, however, no limitations with respect to the types of Gaussian basis sets that can be used (segmented or generally contracted with spherical-harmonic or Cartesian components). In addition to the calculation NMR shieldings and indirect spin–spin couplings at the GGA and hybrid levels, DALTON is capable of calculating DFT molecular gradients as well as DFT singlet and triplet excitation energies at the RPA level.

In principle, the only modifications needed to turn a Hartree–Fock code into a DFT code is to replace the Hartree–Fock exchange contributions to the energy and other quantities such as the Fock matrix by the corresponding exchange-correlation contributions of DFT. In hybrid theories, the Hartree–Fock exchange is not completely removed but rather scaled by some factor. Since the perturbing operators (7)–(10) are one-electron operators, all quantities involving these operators in Kohn–Sham theory are formally identical to those in Hartree–Fock theory. The only modifications needed for the calculation of spin–spin coupling con-

TABLE I. Indirect nuclear spin–spin coupling constants (Hz). All calculations have been carried out at the equilibrium geometry in the HIII basis, except as noted for some MCSCF calculations. In the MCSCF calculations, a 6331 CAS was used except that RAS was used for HCN and full-valence CAS for H_2 and C_2H_4. All experimental results are vibrationally averaged except for H_2, HF, and CH_4, for which R_e values are used.

		RHF	LDA	BLYP	B3LYP	CAS	exp.
H_2	H–D	47.3	29.5	44.6	42.6	36.9	41.1[a]
HF	^{19}F–H	632.7	385.5	373.3	419.5	517.7[b]	500±20[c]
H_2O	^{17}O–H	−97.1	−62.3	−67.8	−71.8	−74.5[b]	−80.6[d]
NH_3	^{14}N–H	51.9	34.9	41.8	42.4	42.3[e]	43.6[f]
CH_4	^{13}C–H	146.1	94.0	123.1	122.4	116.7[e]	120.9[g]
HCN	^{15}N–^{13}C	−119.7	−7.9	−11.7	−17.2	−19.8[b]	−18.5[h]
N_2	^{14}N–^{15}N	−15.0	3.9	2.9	1.6	0.8[i]	1.8[j]
CO	^{13}C–^{7}O	−5.0	26.1	22.8	19.5	16.1[i]	16.4[k]
C_2H_4	^{13}C–^{13}C	1235.9	49.9	66.1	70.1	75.7[l]	67.5[m]
mean err.	Hz	127.2	−15.4	−4.5	−7.0	2.2	
mean abs. err.	Hz	170.7	24.4	24.1	11.2	4.9	
stand. dev.	Hz	395.7	39.9	49.0	27.7	7.2	
mean err.	%	119.1	−2.6	12.3	−2.3	−6.5	
mean abs. err.	%	409.7	41.7	30.5	8.4	11.6	
stand. dev.	%	722.9	54.5	40.3	10.6	19.7	

[a]References 13 and 21.
[b]Reference 20.
[c]References 22 and 23.
[d]Reference 24.
[e]HIV basis, Ref. 2.
[f]Reference 25.
[g]Reference 26.
[h]Reference 27.
[i]$12s7p3d/8s4p3d$ basis, Ref. 28.
[j]Reference 29.
[k]Reference 30.
[l]$qz+2d1f$ basis, Ref. 2.
[m]Reference 31.

stants therefore occur in the solution of the response equations, in order to take into account the contributions from the exchange-correlation potential to the singlet and triplet Hessians. We do not derive these contributions here since these are the same as those that occur in DFT RPA theory, which have been described elsewhere.[5] Our implementation of the exchange-correlation contributions to the electronic Hessian has been tested by comparing the DFT RPA singlet and triplet excitation energies obtained by DALTON with those obtained by CADPAC. Since the calculation of the DFT indirect spin–spin coupling constants otherwise uses the same DALTON routines as for Hartree–Fock calculations, we are confident that the calculated DFT indirect spin–spin coupling constants are correct.

III. CALCULATIONS

A. The performance of LDA, BLYP, and B3LYP

In this section, we compare the LDA, BLYP, and B3LYP indirect spin–spin coupling constants with the experimental ones and with those obtained at the Hartree–Fock and CASSCF (complete active space self-consistent field) levels [RASSCF (restricted active space self-consistent field) for HCN]. The CASSCF level was chosen as being typical of a fairly simple yet qualitatively correct *ab initio* level; in Sec. III E, comparisons will be made with other levels of *ab initio* theory.

Except as noted for some of the MCSCF calculations, all calculations have been carried out at the experimental geometries in the HIII basis,[16,17] containing $[7s6p2d]$ contracted spherical-harmonic AOs (atomic orbitals) on each nonhydrogen atom and $[4s2p]$ AOs on each hydrogen atom. This basis is commonly used for NMR shieldings and often also for spin–spin coupling constants.[2] However, since the FC operator (which contains the Dirac delta function) contributes to the spin–spin couplings but not to the shieldings, the basis-set requirements for the spin–spin coupling constants are more stringent.[18–20] As discussed in Sec. III B, the popular HIII basis may therefore not be sufficiently flexible for an accurate calculation spin–spin coupling constants. Still, for the initial comparison of the different schemes in Table I, we shall use the HIII basis. (The slightly larger HIV basis has been used in some of the CASSCF calculations in Table I; the differences between HIII and HIV are small and do not invalidate the comparison.)

In comparing the spin–spin couplings with experiment, one should bear in mind that the vibrational contributions to the experimentally observed coupling constants are mostly unknown. In our comparison, we use the experimental equilibrium values where these are available (for H_2, HF, and CH_4); otherwise, we have used the directly observed (vibrationally averaged) couplings. We note that the vibrational contribution can sometimes be substantial—in HF, for example, the zero-point vibrational correction increases the indirect spin–spin coupling by about 25 Hz (5%).[23]

From the results in Table I, it is clear that the calculated DFT spin–spin coupling constants represent a significant improvement on the Hartree–Fock constants. For example, the CC coupling of C_2H_4 is reduced from 1236 Hz at the Hartree–Fock level to 50 Hz at the LDA level, in fair agreement with the experimental value of 68 Hz. Similar improvements are observed for the CN coupling in HCN and for the couplings in N_2 and CO, all of which are poorly described at the Hartree–Fock level. In short, as we argued earlier, most of the severe problems associated with the poor description of the triplet perturbations at the Hartree–Fock level are

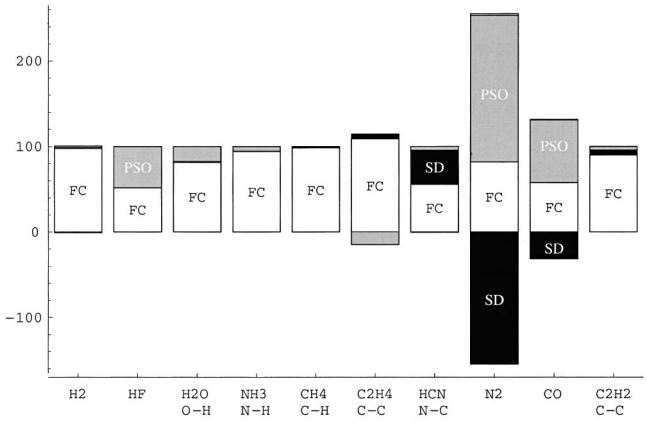

FIG. 1. The relative contributions to the indirect nuclear spin–spin coupling constants as calculated at the B3LYP/HIII level at experimental geometries. The DSO contribution is always small but noticeable at the top of the column for the N_2 molecule.

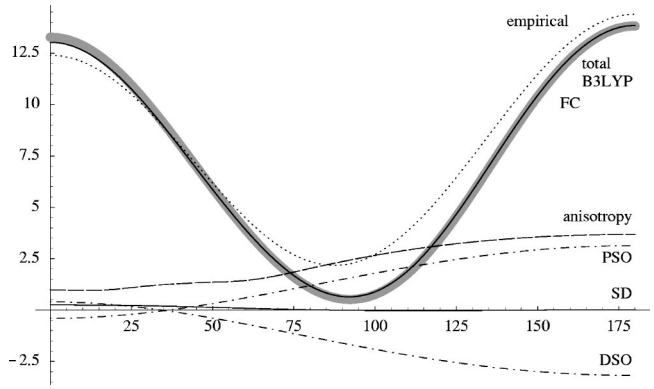

FIG. 2. The Karplus curve calculated at the B3LYP/HIII level compared with the empirical Durette–Horton curve. The Durette–Horton curve has been obtained by plotting (17); the B3LYP curves have been obtained by third-order polynomial fittings to successive calculated points for $\phi = 0°, 10°, \ldots, 180°$.

solved at the LDA level. We also note that, whereas the Hartree–Fock model always overestimates the coupling (usually very significantly), the LDA model mostly underestimates it.

Passing on to the gradient-corrected BLYP level, the couplings usually increase, improving the agreement with experiment somewhat. Nevertheless, the agreement is far from satisfactory, the BLYP mean absolute errors being 24 Hz and 31%. At the B3LYP level, however, there is a significant improvement in the calculated couplings, with mean absolute errors of 11 Hz and 8%; the corresponding CASSCF errors being 5 Hz and 12%. These seemingly contradictory errors illustrate the difficulties associated with judging the errors of calculated spin–spin coupling constants. Whereas CASSCF is better than B3LYP in absolute terms because of a large B3LYP error of 90 Hz for HF, B3LYP is better than CASSCF in relative terms because of a large CASSCF error of 100% for N_2. Ignoring the HF coupling, the B3LYP mean absolute error is 2.7 Hz. Thus, with the reservation that B3LYP severely underestimates the coupling in HF, we conclude that it performs very well for the calculation of indirect spin–spin couplings—for molecules containing a variety of chemical bonds between first-row atoms.

B. The relative importance of the contributions to the coupling constants

The cost of evaluating the indirect spin–spin coupling constants is significantly reduced if we omit the SD contributions. Indeed, in some applications, all contributions except the FC contribution are omitted, reducing the cost of the calculation by several factors. In Fig. 1, we have plotted the four contributions to the B3LYP/HIII couplings at the experimental geometries. Although the FC contribution dominates in most cases [partly because of the large prefactor in (9), which is squared in the calculated couplings], this is not always so. For example, in HF, the PSO contribution is as large as the FC contribution; moreover, in N_2, the PSO contribution is more than twice as large as the FC contribution and the SD contribution as large as the PSO contribution but of opposite sign. The SD mechanism also makes significant contributions in HCN and CO. The DSO contribution is the least important but it is sometimes as large as the PSO contribution—see the discussion of the Karplus curve later.

In short, none of the coupling mechanisms that arise in Ramsey's theory can be *a priori* neglected in accurate studies of spin–spin couplings. However, significant savings can sometimes be gained by carrying out pilot calculations in a small basis and only the dominant contributions—usually the FC contribution—in a large basis. This approach makes sense since the FC contribution is usually more sensitive to the quality of the basis than the other contributions.

C. Basis-set saturation

It is well established that the quality of the calculated indirect spin–spin couplings depends critically on the flexibility of the one-electron basis.[18–20] This sensitivity arises from the presence of the Dirac delta function in the FC operator, which appears to second-order in the coupling constants. Clearly, for the accurate calculation of indirect spin–spin coupling constants, we must provide a flexible description of the core. However, it is also apparent from the form of the FC operator that sufficient flexibility is obtained by decontracting the *s* functions and by augmenting the original energy-optimized basis with steep *s* functions, usually added as an even-tempered extension to the functions present in the original basis set.

In Table II, we have listed the B3LYP couplings calculated with such augmented basis sets. Whereas the effect of decontraction is mostly small (except in the hydrocarbons), the effect of adding steep *s* functions is significant. For HF and H_2O, the augmentation brings the calculated B3LYP couplings into better agreement with experiment; for H_2, CH_4, and C_2H_2, the agreement with experiment becomes poorer. Clearly, for a useful comparison and evaluation of the different computational methods, basis sets larger than HIII should be used. In our comparison with other methods in Sec. III E, we have used both the HIII basis and the HIII-*su*3 basis (in which the original *s* functions have been decontracted and augmented with three steep functions).

TABLE II. Basis-set convergence of the B3LYP indirect nuclear spin–spin coupling constants at the experimental geometries (Hz).

	H_2 H–D	HF ^{19}F–H	H_2O ^{17}O–H	NH_3 ^{14}N–H	CH_4 ^{13}C–H	HCN ^{13}C–^{15}N	N_2 ^{14}N–^{15}N	CO ^{13}C–^{17}O	C_2H_2 ^{13}C–^{13}C	C_2H_4 ^{13}C–^{13}C
HIII	42.6	419.5	−71.8	42.4	122.4	−17.2	1.6	19.5	200.8	70.1
uncontracted	42.8	419.1	−71.3	41.7	120.6	−17.2	1.5	18.9	195.8	68.5
1 *s* added	46.6	431.1	−74.7	44.0	127.8	−17.6	1.6	19.3	201.4	71.0
2 *s* added	48.3	437.5	−76.3	45.1	131.1	−17.7	1.6	19.4	204.0	72.1
3 *s* added	48.9	439.3	−76.8	45.4	132.2	−17.7	1.6	19.5	204.9	72.4
Experimental	41.1	500	−80.6	43.6	120.9	−18.5	1.8	16.4	184.5	67.5

D. Rescaling of exact exchange

It has been found that, for NMR shieldings, a reoptimization of the exact Hartree–Fock exchange in B3LYP significantly improves the agreement between calculated and experimental shieldings.[32] In particular, if the Kohn–Sham orbitals are first optimized at the B3LYP level with 5% exact Hartree–Fock exchange (rather than 20%), then a subsequent calculation of shieldings in an uncoupled sum-over-states GGA fashion yields results that differ from the observed ones by only a few percent.[14,32] In view of the success of this approach, we have investigated the effect of changing the amount of exact Hartree–Fock exchange in the calculation of spin–spin coupling constants.

In Table III, we have listed the indirect spin–spin coupling constants as calculated at the B3LYP/HIII level with different amounts of exact exchange: 15%, 20% (true B3LYP) and 25%. From these results, it appears that the spin–spin coupling constants cannot be improved simply by rescaling the Hartree–Fock exchange. The mean absolute errors are 12.5, 11.7, and 11.2 Hz, respectively, for 15%, 20%, and 25% exact exchange (ignoring the HF molecule, the errors become 3.8, 4.1, and 4.6 Hz); in relative terms, the errors are 10.1%, 8.4%, and 10.2%. In short, the mean absolute errors are not much affected by the rescaling; if anything, the best results are obtained with the true B3LYP functional. We conclude that any reoptimization of the empirical parameters in B3LYP must be carried out in a manner more general than that attempted here (i.e., by changing all parameters) but is not likely to lead to a significant improvement on the original functional.

E. Comparison of B3LYP with other methods

Having established that B3LYP performs better than LDA and BLYP with respect to the accurate calculation of indirect spin–spin coupling constants, we now compare B3LYP with available *ab initio* data from the literature—in particular, with MCSCF calculations and with SOPPA(CCSD) (second-order polarization propagator approximation with CCSD amplitudes)[33] and CCSD (coupled-cluster singles-and-doubles)[34] calculations. In addition, comparisons are made with previous DFT calculations by Malkin *et al.*[3] In their DFT calculations, these authors have used the Perdew and Wang exchange functional[35] with the Perdew correlation functional[36] (PP) and ignored the SD contribution to the couplings.

In Table IV, we have listed the coupling constants calculated for a variety of molecular systems at different levels of theory. One difficulty with the comparison of the different methods is the basis set, which is not the same in all cases. While this circumstance complicates the picture, it should be recalled that the requirement on the basis set varies considerably among the different methods—being, for example, much more stringent for CCSD calculations than for restricted Hartree–Fock (RHF) calculations. Still, the requirements with respect to the saturation of the inner *s* core space are the same for all methods. As demonstrated in Sec. III C, it would be preferable to use basis sets of at least HIII-*su*3 quality in all calculations. However, many of the spin–spin coupling constants reported in the literature have not been calculated with this basis. For this reason, we have in Table IV listed the B3LYP couplings calculated using both the HIII basis and the HIII-*su*3 basis. Finally, we note that, for some of the coupling constants in Table IV (in particular those calculated at the CCSD and PP levels), not all contributions have been included, further complicating the comparison.

A comparison of the spin–spin coupling constants in Table IV reveals that the B3LYP method provides spin–spin coupling constants that rival those of CASSCF and CCSD but not quite those of RASSCF and SOPPA(CCSD). In absolute terms (Hz), the worst DFT performance is observed for the HF molecule, which seems to be a particularly hard case for DFT but does not present difficulties for the *ab initio*

TABLE III. The indirect spin–spin coupling constants calculated at the B3LYP/HIII level with 15% exact Hartree–Fock exchange, 20% exact exchange (true B3LYP) and 25% exact exchange (Hz).

	H_2 H–D	HF ^{19}F–H	H_2O ^{17}O–H	NH_3 ^{14}N–H	CH_4 ^{13}C–H	HCN ^{13}C–^{15}N	N_2 ^{14}N–^{15}N	CO ^{13}C–^{17}O	C_2H_2 ^{13}C–^{13}C	C_2H_4 ^{13}C–^{13}C
15%	42.0	409.1	−70.5	41.7	120.4	−15.4	2.1	20.6	197.7	67.6
20%	42.6	419.5	−71.8	42.4	122.4	−17.2	1.6	19.5	200.8	70.1
25%	43.3	430.1	−73.2	43.0	124.5	−19.1	1.2	18.3	204.0	72.7
exp.	41.1	500	−80.6	43.6	120.9	−18.5	1.8	16.4	184.5	67.5

TABLE IV. Comparison of B3LYP indirect spin–spin coupling constants with *ab initio* coupling constants and with PP DFT coupling constants (Hz).

		RHF HIII	CAS	RAS	SOPPA (CCSD)	CCSD	PP HIII	B3LYP HIII	B3LYP HIII-su3	exp.
HF	$^1J_{FH}$	632.7	542.6[a]	529.1[b]	529.4[c]	513.4[d]	396.2[e]	419.5	439.3	500±20[f]
H_2O	$^1J_{OH}$	−97.1	−83.9[a]	−77.1[g]	−80.6[c]	−74.9[d]	−56.2[e]	−71.8	−76.8	−80.6[h]
	$^2J_{HH}$	−20.7	−9.6[a]	−12.6[g]	−8.8[c]	−10.8[d]		−7.1	−8.1	−7.11[h]
NH_3	$^1J_{NH}$	51.9	42.3[i]		44.3*	41.8[d]	36.9[e]	42.4	45.4	43.6[j]
	$^2J_{HH}$	−21.9	−9.8[i]		−11.3*	−12.1[d]		−8.9	−9.8	−10.0[j]
CH_4	$^1J_{CH}$	146.1	116.7[i]	121.9[k]	122.3[c]		121.6[e]	122.4	132.2	120.9[l]
	$^2J_{HH}$	−23.7	−13.2[i]	−13.6[k]	−14.0[c]		−10.6[e]	−11.1	−13.3	−12.0[l]
N_2	$^1J_{NN}$	−15.3	0.5[m]	0.8[m]	2.1[c]		4.7[e]	1.6	1.6	1.8[n]
CO	$^1J_{CO}$	−5.0	11.5[m]	16.1[m]	18.6[c]		25.9[e]	19.5	19.5	16.4[o]
C_2H_2	$^1J_{CC}$	353.3	187.7[p]	182.6[q]	190.0[r]	166.2[s]	184.3[e]	200.8	204.9	184.5[t]
	$^1J_{CH}$	379.8	238.5[p]	241.4[q]	254.9[r]	226.7[s]	249.1[e]	253.8	274.0	242.4[t]
	$^2J_{CH}$	−51.0	47.0[p]	49.2[q]	51.7[r]	43.2[s]	49.1[e]	52.2	55.9	53.8[t]
	$^3J_{HH}$	70.6	12.1[p]	12.6[q]	11.3[r]	7.6[s]	9.0[e]	10.3	11.0	10.1[t]
C_2H_4	$^1J_{CC}$	1235.9	75.7[i]	69.5[i]	70.1**	70.1[u]	61.2[e]	70.1	72.4	67.5[v]
	$^1J_{CH}$	688.7	155.7[i]	154.0[i]	157.2**	153.2[u]	152.0[e]	154.2	166.7	156.3[v]
	$^2J_{CH}$	−519.0	−5.8[i]	−3.0[i]	−3.1**	−3.0[u]	−0.7[e]	−1.3	−1.5	−2.4[v]
	$^2J_{HH}$	−296.4	−2.4[i]	1.3[i]	1.0**	0.4[u]	4.3[e]	3.2	3.8	2.4[v]
	$^3J_{cis}$	304.6	12.4[i]	11.6[i]	17.8**	11.6[u]	10.1[e]	11.0	13.0	11.7[v]
	$^3J_{trans}$	343.9	18.4[i]	18.5[i]	24.7**	17.8[u]	16.9[e]	17.7	20.0	19.0[v]

[a]Reference 20.
[b]Reference 23, 544.2 Hz in Ref. 37.
[c]Reference 33.
[d]EOM-CCSD Ref. 34.
[e]Only FC for H_2O and NH_3, SD ignored in all cases, Ref. 3.
[f]R_e value, Refs. 22 and 23.
[g]Reference 38.
[h]Reference 24.
[i]Reference 2.
[j]Reference 25.
[k]Reference 39.
[l]R_e value, Ref. 26.
[m]Reference 28.
[n]Reference 29.
[o]Reference 30.
[p]Reference 40.
[q]Reference 41, see also Ref. 31.
[r]Reference 42.
[s]Reference 43.
[t]R_e value, Ref. 42.
[u]Reference 44.
[v]Reference 31.
*Added in proof, Reference 51.
**Added in proof, Reference 52.

methods; observing the same difficulties in their PP calculations, Malkin *et al.* related these to the large number of lone pairs in HF.[3] For the PP calculations in Table IV, omission of the SD contribution leads to poor results for HF, CO, and N_2. The latter two molecules are well described at the B3LYP level, in particular in comparison with the CAS model. It is also gratifying to note that, for the unsaturated hydrocarbons C_2H_2 and C_2H_4, the full set of spin–spin coupling constants—that is, the one-bond, geminal, and vicinal couplings—are well reproduced at the B3LYP level, with an unambiguous one-to-one correspondence between the observed and calculated coupling constants.

F. The Karplus relation

The indirect nuclear spin–spin coupling constants are sensitive to details of molecular structure and conformation, as illustrated by the famous Karplus relationship between vicinal coupling constants and the dihedral angle ϕ between two CH bonds.[45] In its simplest form, the Karplus equation may be expressed as

$$^3J(\phi) = C_0 + C_1 \cos\phi + C_2 \cos(2\phi), \tag{15}$$

where $^3J(\phi)$ is the coupling constant between two hydrogen atoms on neighboring carbon atoms. In Fig. 2, we have plotted the Karplus curve for ethane (in Hz) as calculated at the B3LYP level in the HIII basis. For comparison, we have included the empirical Durette–Horton curve.[46] We note, however, that several (similar) Karplus curves exist in the literature;[47–49] Refs. 48 and 49 also contain Karplus curves calculated at the Hartree–Fock level.

The B3LYP curve is remarkably similar to the empirical Karplus curve. In terms of the Fourier expansion (15), these curves may be expressed as

$$^3J(\phi)_{\mathrm{B3LYP}} = 7.0 - 0.1\cos\phi + 6.5\cos(2\phi), \tag{16}$$

$$^3J(\phi)_{\mathrm{DH}} = 7.8 - 1.0\cos\phi + 5.6\cos(2\phi). \tag{17}$$

Whereas the Durette–Horton curve is defined by the relation (17) and obtained by adjusting to the observed spin–spin coupling constants of ethanelike molecules, the B3LYP curve (16) has been obtained by fitting the calculated vicinal spin–spin coupling constants of ethane for the 19 torsional angles 0°, 10°, ..., 180° to the three-term expansion (15). We note that the Karplus relation is completely dominated by the FC contribution, which depends critically on the dihedral angle; the SD contribution is small and the DSO and PSO contributions very nearly cancel. The near cancellation of the orbital contributions is a common feature of vicinal H–H couplings—see, for example, the discussion in Ref. 50. For B3LYP, the minimum in the Karplus curve occurs at 92.2°. In conclusion, it appears that B3LYP represents an excellent model for the study of Karplus-type conformational relations in NMR spectroscopy.

IV. CONCLUSIONS

We have presented an implementation of indirect nuclear spin–spin coupling constants at the DFT level for GGA and hybrid functionals. The first applications of this method to the calculation of spin–spin coupling constants are promising, suggesting that the hybrid B3LYP functional gives results whose accuracy matches that of the best *ab initio* results in the literature. Compared with experiment, the errors are typically 10% although a more careful analysis is necessary to establish the effects of basis-set incompleteness and vibrational averaging. If anything, the errors observed for the spin–spin couplings in our applications are smaller than those of the shielding constants calculated at the same level of theory, suggesting that B3LYP provides a useful tool for the theoretical study of NMR spectra. Bearing in mind that the B3LYP model can easily be applied to large systems—much larger than those studied by high-level *ab initio* methods—it appears that we now for the first time have at our disposal a useful tool for the study of NMR shielding and spin–spin coupling constants of large organic molecules. The results obtained at the LDA and BLYP levels are poorer than those obtained at the B3LYP level, with errors often several times larger (in particular at the LDA level). Still, even the simple LDA functional displays none of the instability problems characteristic of the Hartree–Fock model, suggesting that the crude effects of static correlation are included already at this simple level of theory.

Note added in proof. Recently, V. Sychrovsky, F. Gräfenstein, and D. Cremer have presented an independent analytical implementation of indirect spin–spin coupling constants at the GGA and hybrid levels of nonrelativistic DFT, see Ref. 53. Their findings and conclusions agree with ours, demonstrating that the evaluation of NMR spin–spin coupling constants by DFT is a potentially high-accuracy semi-empirical approach. A discrepancy occurs for C_2H_4 since Sychrovsky *et al.* have used an incorrect geometry for this molecule, with the values for the HCH and HCC bond angles interchanged.

ACKNOWLEDGMENTS

This work has been supported by the Norwegian Research Council (NFR). We would like to thank Roger Amos, Michal Jaszunski, Kenneth Ruud, Trond Saue, and Stephan Sauer for discussions and comments, and for providing us with their results prior to publication.

[1] N. F. Ramsey, Phys. Rev. **91**, 303 (1953).
[2] T. Helgaker, M. Jaszunski, and K. Ruud, Chem. Rev. **99**, 293 (1999).
[3] V. G. Malkin, O. L. Malkina, and D. R. Salahub, Chem. Phys. Lett. **221**, 91 (1994).
[4] R. M. Dickson and T. Ziegler, J. Phys. Chem. **100**, 5286 (1996).
[5] R. Bauernschmitt and R. Ahlrichs, Chem. Phys. Lett. **256**, 454 (1996).
[6] S. J. Vosko, L. Wilk, and M. Nusair, Can. J. Phys. **58**, 1200 (1980).
[7] A. D. Becke, Phys. Rev. A **38**, 3098 (1988).
[8] C. Lee, W. Yang, and R. G. Parr, Phys. Rev. B **37**, 785 (1988).
[9] A. D. Becke, J. Chem. Phys. **98**, 5648 (1993).
[10] P. J. Stephens, F. J. Devlin, C. F. Chabalowski, and M. J. Frisch, J. Chem. Phys. **98**, 11623 (1994).
[11] J. Autschbach and T. Ziegler, J. Chem. Phys. **113**, 939 (2000).
[12] T. Helgaker, H. J. Aa. Jensen, P. Jørgensen *et al.*, DALTON, an electronic structure program, Release 1.0.
[13] O. Vahtras, H. Ågren, P. Jørgensen, H. J. Aa. Jensen, S. B. Padkjaer, and T. Helgaker, J. Chem. Phys. **96**, 6120 (1992).
[14] T. Helgaker, P. J. Wilson, R. D. Amos and N. C. Handy, J. Chem. Phys. **113**, 2983 (2000).
[15] CADPAC6.5., R. D. Amos, I. L. Alberts, J. S. Andrews *et al.*, The Cambridge Analytic Derivatives Package 1998.
[16] S. Huzinaga, *Approximate atomic functions* (University of Alberta, Edmonton, 1971).
[17] S. Huzinaga, J. Chem. Phys. **42**, 1293 (1965).
[18] J. Oddershede, J. Geertsen, and G. E. Scuseria, J. Phys. Chem. **92**, 3056 (1988).
[19] J. Geertsen, J. Oddershede, W. T. Raynes, and G. E. Scuseria, J. Magn. Reson. **93**, 458 (1991).
[20] T. Helgaker, M. Jaszunski, K. Ruud, and A. Gorska, Theor. Chem. Acc. **99**, 175 (1998).
[21] Y. I. Neronov and A. E. Barsach, Zh. Eksp. Teor. Fiz. **69**, 1872 (1975).
[22] S. M. Bass, R. L. DeLeon, and J. S. Muenter, J. Chem. Phys. **86**, 4305 (1987); J. S. Muenter and W. Klemperer, *ibid.* **52**, 6033 (1970).
[23] P.-O. Åstrand, K. Ruud, K. V. Mikkelsen, and T. Helgaker, J. Chem. Phys. **110**, 9463 (1999).
[24] N. M. Sergeyev, N. D. Sergeyeva, Y. A. Strelenko, and W. T. Raynes, Chem. Phys. Lett. **277**, 142 (1997).
[25] R. A. Bernheim and H. Batiz-Hernandez, J. Chem. Phys. **40**, 3446 (1964).
[26] B. Bennett, W. T. Raynes, and C. W. Anderson, Spectrochim. Acta, Part A **45**, 821 (1989); F. A. L. Anet and D. J. O'Leary, Tetrahedron Lett. **30**, 2755 (1989).
[27] G. Dombi, P. Diehl, J. Lounila, and R. Wasser, Org. Magn. Reson. **22**, 573 (1984).
[28] O. Vahtras, H. Ågren, P. Jørgensen, T. Helgaker, and H. J. Aa. Jensen, Chem. Phys. Lett. **209**, 201 (1993).
[29] J. O. Friedrich and R. E. Wasylishen, J. Chem. Phys. **83**, 3707 (1985).
[30] R. E. Wasylishen, J. O. Friedrich, S. Mooibroek, and J. B. Macdonald, J. Chem. Phys. **83**, 548 (1985).
[31] J. Kaski, P. Lantto, J. Vaara, and J. Jokisaari, J. Am. Chem. Soc. **120**, 3993 (1998).
[32] P. J. Wilson, R. D. Amos, and N. C. Handy, Chem. Phys. Lett. **312**, 475 (1999).
[33] T. Enevoldsen, J. Oddershede, and S. P. A. Sauer, Theor. Chem. Acc. **100**, 275 (1998).
[34] S. A. Perera, H. Sekino, and R. J. Bartlett, J. Chem. Phys. **101**, 2186 (1994).
[35] J. P. Perdew and Y. Wang, Phys. Rev. B **33**, 8800 (1986).
[36] J. P. Perdew, Phys. Rev. B **33**, 8822 (1986); **34**, 7406 (1986).
[37] J. San Fabián, J. Casanueva, E. San Fabián, and J. Guilleme, J. Chem. Phys. **112**, 4143 (2000).
[38] M. Pecul and J. Sadlej, Chem. Phys. Lett. **308**, 486 (1999).
[39] J. Guilleme and J. San Fabián, J. Chem. Phys. **109**, 8168 (1998).
[40] M. Pecul and J. Sadlej, Chem. Phys. **234**, 111 (1998).
[41] M. Jaszunski and K. Ruud (in preparation).
[42] R. D. Wigglesworth, W. T. Raynes, S. Kirpekar, J. Oddershede, S. P. A. Sauer, J. Chem. Phys. **112**, 3735 (2000).
[43] S. A. Perera, M. Nooijen, and R. J. Bartlett, J. Chem. Phys. **104**, 3290 (1996).
[44] H. Sekino and R. J. Bartlett, Chem. Phys. Lett. **225**, 486 (1994).
[45] M. Karplus, J. Chem. Phys. **30**, 11 (1959).
[46] P. L. Durette and D. Horton, Org. Magn. Reson. **3**, 417 (1971).
[47] C. A. G. Haasnoot, F. A. A. M. de Leeuw, and C. Altona, Tetrahedron **36**, 2783 (1980).
[48] J. San-Fabian, J. Guilleme, E. Diez, P. Lazzeretti, M. Malagoli, and R. Zanasi, Chem. Phys. Lett. **206**, 253 (1993).
[49] J. San-Fabian, J. Guilleme, E. Diez, P. Lazzeretti, M. Malagoli, R. Zanasi, A. L. Esteban, and F. Mora, Mol. Phys. **82**, 913 (1994).
[50] G. E. Scuseria, Chem. Phys. **107**, 417 (1986).
[51] S. P. A. Sauer, I. Paidarova, and V. Spirko (unpublished).
[52] P. F. Provasi, G. A. Aucar, and S. P. A. Sauer (unpublished).
[53] V. Sychrovsky, J. Gräfenstein, and D. Cremer, J. Chem. Phys. **113**, 3530 (2000).